Journal of Petroleum Science and Engineering 198 (2021) 108164

Contents lists available at ScienceDirect

Journal of Petroleum Science and Engineering

journal homepage: http://www.elsevier.com/locate/petrol

Validation study of water weakening research from outcrop chalks performed on Eldfisk reservoir cores

Emanuela I. Kallesten [a,b,*], Yosra Cherif [a], Merete V. Madland [a,b], Reidar I. Korsnes [a,b], Edvard Omdal [c], Pål Østebø Andersen [a,b], Udo Zimmermann [a,b]

[a] University of Stavanger, Kristine Bonnevies vei 22, 4021, Stavanger, Norway
[b] The National IOR Centre of Norway, University of Stavanger, Kristine Bonnevies vei 22, 4021, Stavanger, Norway
[c] ConocoPhillips, Ekofiskveien 35, 4056, Tananger, Norway

ARTICLE INFO

Keywords:
Reservoir chalk
Waterflooding
Enhanced oil recovery
Creep compaction
Testing at reservoir conditions

ABSTRACT

Seawater injection for Enhanced Oil Recovery (EOR) purposes can increase the hydrocarbon recovery factor in carbonate reservoirs but are also responsible for weakening their mechanical strength. This study investigates the geomechanical behavior of oil-bearing reservoir chalk subject to reactive flow at reservoir conditions. The obtained results are compared with previous results from experiments on water-saturated outcrop chalks.

Two unwashed oil-bearing reservoir chalk cores from the Eldfisk Field in the North Sea are mechanically tested in a triaxial cell. The cores are saturated with NaCl brine prior to testing, in addition to residual oil. The cores' axial and radial deformations were monitored during hydrostatic stress loading and creep under constant 50 MPa stress, at 130 °C. During the test, the cores were flooded with 0.657 M NaCl, 0.219 M $MgCl_2$, 0.219 M $MgCl_2$ + 0.130 M $CaCl_2$ and synthetic seawater (SSW). The average creep strain increased from 0.03% to 0.04% per day radially and from 0.03% to 0.06% axially after changing from the NaCl brine to SSW brine. Flooding $MgCl_2$ brine after NaCl increased the average compaction rate from 0.05% to 0.09% per day radially and from 0.04% to 0.07% per day axially. Adding $CaCl_2$ to the $MgCl_2$ brine reduced the average compaction rate from 0.05% per day during $MgCl_2$ injection to 0.02% per day both radially and axially, comparable to reports from outcrop chalk experiments. The brine composition-dependent creep compaction in the core flooding experiments was explained by dissolution of primary calcite, confirmed by Ion Chromatography, and precipitation of secondary Mg-bearing minerals, seen by Scanning Electron Microscopy (SEM) analytics.

Generally, the aforementioned results describing geomechanical behaviors of oil-bearing reservoir chalk cores under hydrostatic stress and thermochemical influence in this study are comparable to those from previous studies on outcrop chalk, thus supporting many years of laboratory research as applicable in the reservoir chalk context.

1. Introduction

Developing Improved Oil Recovery (IOR) techniques is central in the efforts for sustainability and resource optimization on the Norwegian Continental Shelf (NCS). The discovery of the Ekofisk Field in 1969, marked the beginning of remarkable advances in hydrocarbon production from chalk reservoirs in Norway. 50 years after its discovery, it is still one of the most prolific reservoirs on the NCS.

After the Ekofisk field had a peak in production rate from primary recovery by pore pressure depletion, the production rate decreased dramatically. The pore pressure depletion contributed to an increased effective stress (overburden minus pore pressure) in the reservoir. The resulting compaction facilitated hydrocarbon expulsion from the porous chalk, but also lead to seafloor subsidence (Teufel et al., 1991; Sulak and Danielsen, 1988; Hermansen et al., 1997, 2000).

Implementing the seawater injection at Ekofisk Field in 1987 contributed to reservoir re-pressurization and an increase in oil production rates. However, despite re-pressurization of the reservoir, high compaction rates continued in certain areas of the field (Schroeder et al., 1998; Hermansen et al., 2000), indicating that effective stress alone was not the only compaction driving mechanism. The interactions between chalk and the injected non-equilibrium seawater, referred to as water

* Corresponding author. University of Stavanger, Kristine Bonnevies vei 22, 4021 Stavanger, Norway.
E-mail address: emanuela.i.kallesten@uis.no (E.I. Kallesten).

https://doi.org/10.1016/j.petrol.2020.108164
Received 24 June 2020; Received in revised form 16 November 2020; Accepted 18 November 2020
Available online 24 November 2020
0920-4105/© 2020 The Authors. Published by Elsevier B.V. This is an open access article under the CC BY license (http://creativecommons.org/licenses/by/4.0/).

weakening is a likely contributor (Hermansen et al., 2000). Studies demonstrate a two-step water effect on chalk: an abrupt, instantaneous weakening occurring at the first water-chalk contact, followed by a creep-like deformation at a lower, stable rate (Schroeder et al., 1998; Korsnes et al., 2006). The initial, dramatic water weakening step explains much of the continued compaction of Ekofisk field, but the focus of this study is rather on the role of water chemistry in water weakening of chalk. Korsnes et al. (2006) demonstrated that while water weakening occurs regardless of the water composition, the magnitude of induced weakening was more pronounced when injecting seawater than in case of distilled water.

Extensive laboratory studies on water-wet outcrop chalk showed that the chemical interplay between ions in the injected seawater and the rock itself, does indeed affect the geomechanical properties of chalk (Korsnes et al., 2006; Madland et al., 2011; Nermoen et al., 2015; Kallesten et al., 2020a). The processes identified as responsible for changing the geomechanical properties of chalk are chemical and mineralogical alterations that occur in the presence of surface active ions in the seawater, such as Ca^{2+}, Mg^{2+} and SO_4^{2-} through adsorption, calcite dissolution, substitution and new mineral precipitation. The rock, as a result, suffers morphological and textural changes that in the end are responsible for chalk weakening.

Korsnes et al. (2006) related water weakening during seawater flooding of chalk to the substitution of Ca^{2+} at the chalk surface with Mg^{2+} at elevated temperatures. It is suggested that due to the size difference between the two ions (Mg^{2+} is smaller than Ca^{2+}) this substitution is associated with causing structural changes at intergranular contacts which weaken the chalk. Madland et al. (2011) demonstrated that when flooding seawater the dissolution/substitution process not only leads to precipitation of new Mg-bearing minerals, but also anhydrite ($CaSO_4$) given the presence of sulfate molecules. Further, Madland et al. (2011) demonstrated that when injecting seawater or simplified seawater solutions such as $MgCl_2$ in chalk cores, it is likely that the fluid in the pores is undersaturated with respect to calcite and supersaturated with respect to other minerals, which leads to new mineral precipitation. However, the total produced calcium exceeds the limited number of surface sites, which indicates that the ion exchange or substitution does not occur indefinitely, and that dissolution remains the dominating mechanism. Based on this observation, Megawati et al. (2011) investigated the hypothesis that adding sufficiently high calcium concentration to the $MgCl_2$ brine will hinder the calcite dissolution and thus not weaken the chalk. The results confirmed this supposition and they observed that by adding 0.130 mol/L $CaCl_2$ to the 0.219 mol/L $MgCl_2$ flooding brine, representing an increase of calcium concentration by a factor of 10 compared to the seawater composition, lead to a severe reduction in both excess calcium production and creep compaction rate of the chalk. Switching back to a non-equilibrium brine reactivated the calcite dissolution and accelerated the compaction.

Besides dissolution/precipitation processes leading to mineral replacement, the interactions between the pore fluid and the chalk surface may also include adsorption and desorption of surface-active ions (Ahsan and Fabricius, 2010; Megawati et al., 2013; Sachdeva et al., 2019a). Megawati et al. (2013) showed that adsorption of sulfate ions present in seawater on the chalk grains can lead to a negative surface charge that triggers the occurrence of repulsive forces at granular contacts, which consequently reduces the cohesion between grains, weakening the chalk. Nermoen et al. (2018) and Sachdeva et al. (2019a) observed that Mg^{2+} can have a similar effect. Due to the non-equilibrium between $MgCl_2$ brine and calcite surface, magnesium ions adsorb on available chalk surface sites and as calcium ions desorb from the internal surface during flooding until equilibrium is reached. However, adsorption and desorption are considered as limited processes in this case, that occur only within the few first pore volumes of the injected reactive brine because of the finite number of available surface sites (Madland et al., 2011). Thereafter, the changes in magnesium and calcium concentrations in the effluents are dominated by the dissolution and precipitation processes. Both during the early and late time injection periods of $MgCl_2$ injection into outcrop it appears that very similar amounts of excess Ca is produced as Mg is retained (Madland et al., 2011; Megawati et al., 2015; Andersen et al., 2018; Minde et al., 2018). We hypothesize the same will take place with reservoir chalk samples.

In comparison to reactive brines, geochemical analysis from experiments with non-reactive flooding fluid (NaCl) at 130 °C concluded that in the absence of surface-active ions, chemical alterations such as adsorption, dissolution and precipitation of new minerals, are unlikely to occur (Madland et al., 2011; Megawati et al., 2015; Minde et al., 2018; Wang et al., 2018). Nonetheless, NaCl flooding can dissolve calcite if flooded over a long time period, causing morphological changes such as grain rounding (Gautier et al., 2001). This was reported in outcrop chalk studies (Andersen et al., 2018) and according to Megawati et al. (2011) smoothened crystals corners and edges may lower the mechanical intergranular friction, and consequently enhance the creep development with time.

Another aspect in water weakening research is the presence of additional phases besides brine, as the wettability of chalk (whether the grain surfaces are more water-wet or oil-wet) plays an important role in flooding experiments on mechanical strength, geochemical and petrophysical changes and oil production (Strand et al., 2007; Hiorth et al., 2010; Sachdeva et al., 2019b). Sachdeva et al. (2019b) found that water-wet chalk cores were weaker than mixed-wet (some grain surfaces are water-wet and others are oil-wet) when flooded with non-reactive brines (NaCl). However, injecting $MgCl_2$ and SSW lead to increasing creep rates in both water-wet and mixed-wet cores alike, indicating that the presence of oil in the pores does not avert the flooding brine from the intergranular contacts and therefore does not hinder the weakening effects of reactive flow on chalk as described above.

Not least, mineralogy plays an important role in rock-fluid interactions (Andersen et al., 2018; Fabricius and Borre, 2007; Hiorth et al., 2010; Madland et al., 2011; Minde et al., 2018; Strand et al., 2007; Kallesten et al., 2020b). Madland et al. (2011) pointed out that pure chalk (high calcite content) has a slower reaction rate than chalk with higher non-carbonate content (particularly silicates, clays). Therefore, despite the rather predictable mineralogy and petrology of chalk, important aspects such as the depositional environment, stress history, diagenesis, burial depth can strongly influence its engineering properties and a direct transfer of data from outcrop chalk to reservoir chalk is not always appropriate (Scholle, 1977; Brasher and Vagle, 1996; Hjuler and Fabricius, 2007, 2009; Minde et al., 2016). As an example, North Sea offshore chalks are deeply buried, with depths often exceeding 3 km, whereas onshore chalks such as Danish chalks have relative shallow maximum palaeo-burial depths ranging between 500 and 750 m (Japsen, 1998, 2000; Japsen and Bidstrup, 1999).

Most of the chalk research, however, is performed on outcrop chalk, due to the scarcity and high cost of reservoir test material. Yet, in an effort to identify the most suitable outcrop analogues to the North Sea reservoir chalk, studies of chalk from exposures with a comparable mineralogy, permeability, porosity environment and sedimentary age as reservoir chalk concluded that in spite of the mineralogical, diagenetic differences, laboratory tests on certain chalk outcrops can nontheless provide valuable information for further research (Collin et al., 2002; Hjuler and Fabricius, 2009; Jarvis, 2006). The studies recommend outcrop chalk such as the Belgian Liège chalk as a possible mechanical analogue to Ekofisk field and the Danish Aalborg chalk is considered comparable to Valhall reservoir chalk in terms of geo-mechanical properties. Still, the studies urge to careful consideration when selecting suitable outcrop chalk as reservoir chalk substitutes for mechanical testing.

Conducting laboratory tests on actual reservoir chalk cores is a unique opportunity to validate results and behavior seen in laboratory tests on outcrop chalk. For that purpose, this study investigates the behavior of reservoir chalk when tested with procedures giving significant responses in outcrop chalk. The core material is from Eldfisk Field,

the second largest producing field in the Greater Ekofisk area, located in the Southern tip of the NCS. Mineralogically the Eldfisk chalk consists almost entirely of calcite (96–97%), while the non-carbonate phase is mainly quartz, kaolinite and scarce dolomite, feldspar, pyrite, apatite and smectite-illite (Madsen, 2010).

The study will replicate the test conditions used previously on outcrop chalk (Madland et al., 2011; Megawati et al., 2011, 2015; Korsnes et al., 2013; Zimmermann et al., 2015; Andersen et al., 2018; Minde et al., 2018; Nermoen et al., 2018; Wang et al., 2018; Sachdeva et al., 2019b). Two reservoir chalk cores will be tested in triaxial cells under hydrostatic stress conditions, and flooded with NaCl, seawater, $MgCl_2$ and $MgCl_2$ with added $CaCl_2$ (to reduce calcite dissolution) at 130 °C, over several weeks. The focus will be on axial and radial strain measurements in response to hydrostatic loading and creep and variation in flooding brine. Also, the effluent concentrations will be monitored throughout the test by collecting effluent probes regularly, in order to detect possible changes in ionic concentration compared with the concentrations of the injecting fluid. Finally, Scanning Electron Microscopy will investigate the mineralogy and texture of the flooded chalk. The results will allow a direct comparison between reservoir chalk from the North Sea and the outcrop chalk tests in terms of geomechanical behavior and geochemical effects of injecting brine chemistry. Specific research questions we seek to answer are:

- Will $MgCl_2$ brine and seawater, which are reactive to outcrop chalk, also be reactive to Eldfisk reservoir chalk in terms of mineralogical changes?
- Will switching from an inert brine (NaCl) to a reactive brine lead to enhanced compaction during creep?
- Will $MgCl_2$ brine injection, followed by injecting $MgCl_2$ brine with added high $CaCl_2$ concentration result in reduced compaction rate?
- Will Mg^{2+} loss and Ca^{2+} gain be identical when $MgCl_2$ is injected into reservoir chalk?

Knowledge of the reservoir chalk behavior in the same test conditions as the outcrop chalk will verify the relevance of outcrop chalk testing for the North Sea context, will refine the search of an outcrop analogue to reservoir chalk, but also enhance the accuracy of reservoir models relevant to the NCS, and eventually contribute to increase efficiency of the EOR techniques from existing and future chalk reservoirs.

2. Sample set, experimental procedures, and methods

2.1. Sample set

This study focuses on tests performed on two reservoir chalk cores (E2 and E3, Fig. 1) from the Ekofisk Formation (Eldfisk field). Although ideally several cores should be tested, the two cores studied here are a rare opportunity considering the limited availability for laboratory testing and the cost of obtaining reservoir cores. The cores contained saturation of reservoir oil and they have not been exposed to EOR fluids. To maintain the cores as close to their original state as possible, the residual oil and salts were not removed prior to testing. Core E2 contained a visible fissure on the top facet, which did not seem to penetrate the entire core.

To obtain a cylindrical shape with parallel end facets compatible with the testing equipment, the cores' irregular end facets were cut with a Struers Discotom-5 cutting machine and grinded with a Delta LF-350 machine. The excess end pieces were stored for a later study investigating possible mineralogical differences between untested and tested chalk. The porosity of the obtained cylinders was measured by gas pycnometry. Because the cores were unwashed, the measured porosity represents effective values rather than true porosity. The dimensions and porosity of the cores are listed in Table 1.

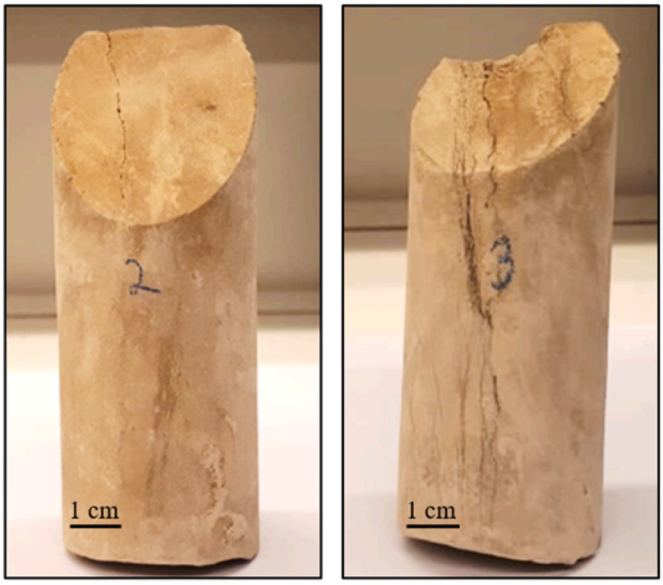

Fig. 1. Chalk cores E2 (left) and E3 (right) before testing.

Table 1
Dimensions and effective porosity of the tested cores.

Core ID	Length [mm]	Diameter [mm]	Effective porosity [%]
E2	53.00	37.93	18.00
E3	52.40	37.98	18.93

2.2. Injecting brines

Four different brines were used for core flooding, henceforth generically identified by and referred to according to their composition: 0.657 M sodium chloride (NaCl), 0.219 M magnesium chloride ($MgCl_2$), 0.219 M magnesium chloride spiked with 0.130 M calcium chloride ($MgCl_2$+$CaCl_2$) and synthetic seawater (SSW). Apart from SSW, the rest of the brines were prepared with distilled water (DW) in equilibrium with calcite. 0.1 g/L calcite powder was added to DW and stirred at room temperature. The solution was then filtered through a 0.22 μm filtrate paper, to remove all undissolved calcite and used further for preparation of the sodium chloride and magnesium chloride brines. The ionic strength of the monosalt brines was set to match the ionic strength of seawater. A summary of the injecting brine compositions is shown in Table 2, discounting calcite equilibration of DW.

Calcite equilibration makes sodium chloride brine inert, thus avoiding textural alteration in contact with chalk. This would provide a contrast in comparison to the reactive brines (magnesium chloride and synthetic seawater) which contain surface-active ions such as Mg^{2+}, Ca^{2+} and SO_4^{2-}, an indication of the effect of rock-fluid interactions when injecting reactive brines through chalk.

Table 2
Chemical composition of the flooding brines; here, ionic composition of sodium chloride and magnesium chloride without considering calcite equilibration.

Injecting brine	NaCl	$MgCl_2$	$MgCl_2$ + $CaCl_2$	SSW
Ionic strength [-]	0.657	0.657	1047	0.657
Cl^- [mole/L]	0.657	0.438	0,698	0.525
Na^+ [mole/L]	0.657			0.450
Mg^{2+} [mole/L]		0.219	0,219	0.045
SO_4^{2-} [mole/L]				0.024
Ca^{2+} [mole/L]			0,130	0.013
HCO_3^- mole/L]				0.002
K^+ [mole/L]				0.010

2.3. Triaxial cell test setup and procedures

Both cores were saturated with NaCl in vacuum conditions before cell mounting and were continuously flooded with the same brine during the first stages of the test (Table 3). The injecting rate was 0.023 ml/min, equivalent of approximately 3 pore volumes (PVs) per day. The effluent brine was collected throughout the test at regular intervals; the first 9–12 PVs (i.e., 3–4 days) after changing to a new brine were sampled 4 times per day, and thereafter once per day. Comparison of the effluent composition to the original injecting brine provides an insight in the rock-fluid interactions during the test.

The triaxial cell is equipped with an outer heating jacket and a regulating system (Omron E5CN) with precise Proportional Integral Derivative (PID) temperature control (±1.0 °C). The system includes two Quizix QX-2000HC pumps that control the axial and confining pressures independently, and a fluid injection pump (Gilson 307HPLC) as well as a backpressure regulator that controls the pore pressure. A schematic diagram representing the triaxial cell setup such as the one used in this study can be found in Nermoen et al. (2016).

During cell mounting, perforated drainage disks with the same diameter as the cores are placed at both brine-saturated core ends to ensure an evenly distributed fluid flow across the core. Additionally, a steel spacer (19.3 mm length) was placed on top to compensate the limited core length. The cores are isolated from the oil bath in the confining chamber by a heat shrinkage sleeve (fluorinated ethylene propylene –FEP, 0.5 mm wall thickness). Throughout the test, any changes in core diameter (radial strain) were measured with an extensometer (GCTS DEF-5000), placed at mid length of the core. An external axial linear variable displacement transducer (LVDT, ±0.05 mm) positioned on top of the cell piston, which is carefully lowered to slight core contact, monitored changes in the cores' length (axial strain). The cell piston applies a 0.55 MPa pressure, to slightly overcome the piston friction, without causing any notable core deformation. NaCl brine flooding started shortly after the triaxial cell mounting was complete and the procedure continued once the differential pressure across the core (measured between the upstream pore line and the downstream) becomes stable. Both tests are performed at 130 °C, representative to the reservoir temperature of Eldfisk field (Cook and Brekke, 2004; Puntervold and Austad, 2008).

At the beginning of the hydrostatic loading, the confining pressure was 1.2 MPa, while the pore pressure was set to 0.7 MPa. For the rest of the test, the pore pressure was kept constant. Hydrostatic loading started with increasing the confining pressure from 1.2 MPa to 50 MPa at a constant 0.1 MPa/min rate. Since with increasing confining pressure the friction associated with the piston also rises, the piston pressure was adjusted accordingly, and finally set to 4.7 MPa.

Once the hydrostatic loading was complete, the pressures were kept constant for the rest of the test, allowing the cores to deform (creep) over several weeks while flooded with different brines. A summary of the stress and flooding sequence for the tests is shown in Table 3.

The core diameter over the length of the core is not constant after testing at hydrostatic stress conditions, and new core bulk volume expected to appear after hydrostatic testing was estimated from the sum of truncated circular cones with diameter D_i measured at height h_i along the core Eqn 1, assuming symmetric radial deformation at each h_i.

$$V_b = \sum_i \frac{\pi h_i}{12}\left(D_i^2 + D_{i+1}^2 + D_i D_{i+1}\right) \quad (1)$$

After testing, both cores were flooded with DW to avoid salt precipitation. Additionally, the cleaning process for core E3 included injection with methanol and toluene to eliminate any possible hydrocarbon residue and prepare for SEM analyses.

Table 3
Duration of each stress phase correlated to flooding sequences for cores E2 and E3.

Injecting Brine	E2		E3	
	Hydrostatic loading [days]	Creep at 50 MPa [days]	Hydrostatic loading [days]	Creep at 50 MPa [days]
NaCl	*0.3*	*6.7*	*0.3*	*6.7*
SSW	-	*19*	-	-
$MgCl_2$	-	-	-	*28*
$MgCl_2$ + $CaCl_2$	-	-	-	*23*
DW	-	*3.0*	-	*3.0*

2.4. Ion chromatography

The ionic concentrations of the injected and produced brines were measured with a Dionex Ion Chromatography System (ICS)-5000⁺. Dionex IonPac AS20 and IonPac CS19 were used as anion and cation exchange columns, respectively. Prior to the analyses, the original brine and effluent samples were diluted 500 times with DW in a Gilson GX-271 dilution machine. The ionic concentrations of Na^+, Cl^-, Mg^{2+}, Ca^{2+} and SO_4^{2-} were measured against standard solutions with known concentrations.

2.5. Electron microscopy

Fresh surfaces of the flooded material from core E3, were examined with Field Emission Gun-Scanning Electron Microscope (Zeiss Supra 35VP FEG-SEM) to obtain visual images of the grains and the rock structure on μm scale. The measurements were performed in high vacuum mode with an accelerating voltage of 15 kV, aperture size of 30 μm, and a working distance between 8 and 9 mm. The electron microscope is equipped with Energy-Dispersive X-Ray Spectroscope (EDS) with a spot size between 1 and 2 μm, which was applied to determine the mineralogical and elemental composition of the analyzed chalk surfaces. The EDS was calibrated after a dolomite standard from "Astimex Standards Limited" before the sample was analyzed.

The dry, tested core was cut in half longitudinally, then one of the halves was cut in four transverse slices, numbered from P1 to P4 from the core inlet to the outlet, respectively. The method focused on a fragment with a fresh surface from slice P1 (inlet), coated with palladium in an Emitech K550 sputtering device.

3. Results

3.1. Mechanical testing

Both cores were tested in the same triaxial cell, following the same stress sequence as described in section 2.4, at 130 °C.

Eldfisk reservoir core E2 was loaded hydrostatically up to 50 MPa while flooding NaCl at an injection rate equal to 3 PVs/day. The axial stress versus axial, radial and volumetric strain are plotted in Fig. 2. The core was compacted both axially (Fig. 2, blue line) and radially (Fig. 2, red line) but did not yield (stress-strain relationship remains linear). The recorded axial and radial strains at the end of this phase were approximately 0.8% and 0.3% respectively. The calculated bulk modulus (K) from the linear slope of axial stress against volumetric strain as shown in Fig. 2 (yellow line), was 3.9 GPa.

NaCl injection continued during the first 6.7 days of the creep phase (Fig. 3). The axial and radial strain rates (percent/day) stabilized at approximately 0.03%/day. The injecting brine was then changed to synthetic seawater, SSW, for the rest of the creep phase.

As Fig. 3 shows, the compaction accelerated shortly after initiating SSW injection (empty markers) compared to the compaction rate during NaCl injection (full markers). Thereafter, the core continued to deform at an almost constant rate until day 21 of creep. Changing the injection brine to SSW increased the average strain rates from 0.03% to 0.04% per

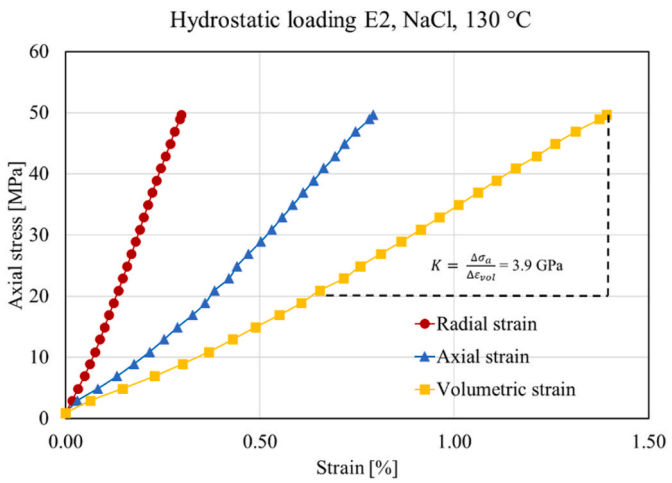

Fig. 2. Stress-strain relationships during hydrostatic loading of core E2.

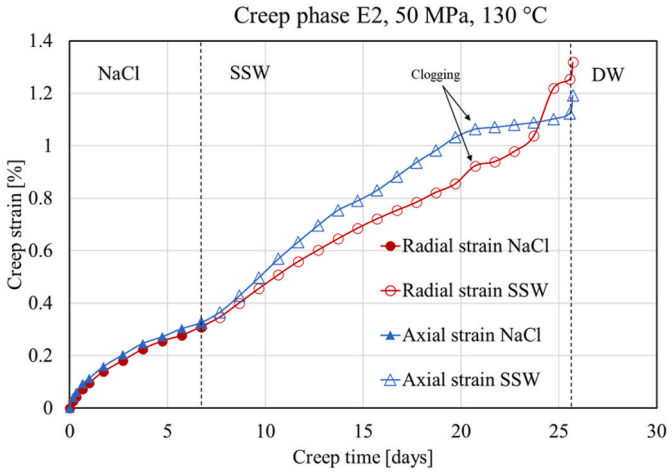

Fig. 3. Axial strain (blue lines) and radial strain (red lines)) for core E2 during NaCl injection (filled markers) and SSW injection (empty markers) during creep at 50 MPa hydrostatic stress. (For interpretation of the references to colour in this figure legend, the reader is referred to the Web version of this article.)

day radially and from 0.03% to 0.06% per day axially, considering the average strain rate for 5 days prior to and after brine change. The flattening of radial and axial creep after day 21 was most likely caused by clogging of the outlet tube. This increased the pore pressure and thereby reduced the effective stress, and consequently the axial deformation rate. This period is not included in the average strain rate evaluation. As soon as the cleaning procedure was initiated with distilled water injection (DW section, Fig. 3), the axial strain rate increased sharply, supporting the assumption of outlet tube clogging due to salt precipitation during flooding. As the precipitates were removed, the pore pressure decreased, the effective stress increased, also inducing a sharp increase in axial strain.

During the first 24 days of creep, E2 deformed more in the axial direction (Fig. 3, blue line) compared to radial (Fig. 3, red line), and more clearly so during SSW injection. However, after 24 days, the radial creep strain accelerated, exceeding the axial strain for the remaining creep period. This unexpected behavior might have been caused by an instrumental error (loosening of the chain of extensometer) or by weakening of the central part of the core.

Mechanical testing of Eldfisk reservoir core E3 started with the same conditions as the previous test, with hydrostatic loading from a confining pressure of 1.2 MPa–50 MPa, while injecting NaCl at a constant 3 PVs/day rate. The axial stress versus axial and radial strains are plotted in Fig. 4. The axial strain (Fig. 4, blue line) and radial strain (Fig. 4, red line) reached 0.86% and 0.69% respectively at the end of the isotropic loading phase. The yield point was not observed for E3. The bulk modulus (K) could be calculated from the linear slope of axial stress versus volumetric strain within the elastic phase as shown in Fig. 4, and it was equal to 2.8 GPa.

The deformation of E3 at constant stress and pore pressure conditions (creep) was studied for 58 days with continuous logging of the axial and radial strains. The creep compaction profile of E3 is shown in Fig. 5. The core was initially flooded with 0.657 M NaCl for the first 6.7 days of creep before flow of 0.219 M $MgCl_2$ started. Axial creep strain (Fig. 5, blue line) and radial creep strain (Fig. 5, red line) at the end of NaCl flow (Fig. 4, full markers) were approximately 0.5%, stabilizing at an average deformation rate of 0.04% per day.

However, the switch to injection of $MgCl_2$ (Fig. 5, empty markers) led to an abrupt increase in the deformation rates both axially and radially. Fig. 5 shows how the radial strain (red line) increased significantly especially until day 22 of creep, then the core continued to deform, but with a lower rate until a strain of 3.2% was recorded. During the same period, the axial strain increased continuously up to 2.1% at 34.7 days. In average, the strain rate per day during the first 5 days of $MgCl_2$ flooding increased compared to the average strain rates during the last 5 days of NaCl injection, from 0.05% to 0.09% radially and from 0.04% to 0.07% axially.

The injection of 0.219 M $MgCl_2$ + 0.130 M $CaCl_2$ (Fig. 5, day 35, cross markers), caused a reduction in the deformation rate compared to the deformation rate while flooding only 0.219 M $MgCl_2$. Comparing the average strain rates over the last $MgCl_2$ injection and the first 10 days after adding $CaCl_2$ to the flooding medium, the compaction rate changed from approximately 0.05%–0.02% per day both radially and axially.

3.2. *Effluent analyses*

The effluent profiles from test E2 focused on the concentrations of the following ions: magnesium, calcium, and sulfate. Fig. 6 shows the ion chromatography analysis of E2, flooded with 0.657 M NaCl and SSW.

During NaCl flooding, the concentrations of sodium and chloride (neither shown) were generally stable throughout the whole experiment with values close to their injected concentration. From the profile of E2, a small magnesium peak of ~0.002 mol/L (Fig. 6, purple line) appeared in the beginning of the creep phase, but it decreased relatively fast and the magnesium concentration in the effluent at this stage stabilized around zero. A larger calcium peak of ~0.01 mol/L (Fig. 6, red line) was observed initially. The calcium concentration also generally decreased, with a brief fluctuation (day 3) and it stabilized at ~ 0.003 mol/L.

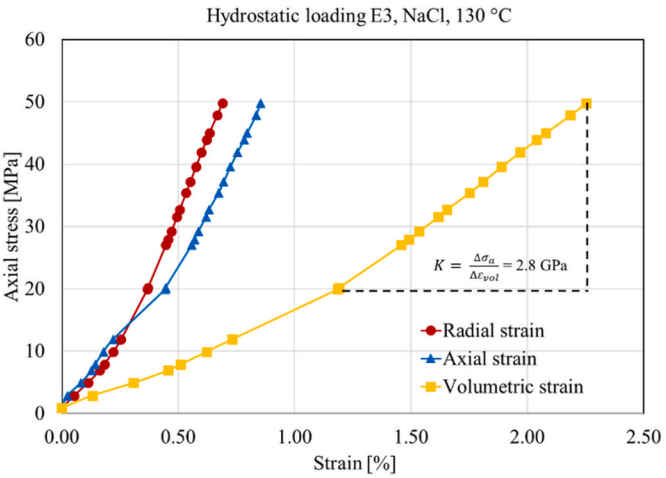

Fig. 4. Stress-strain relationships during hydrostatic loading of core E3.

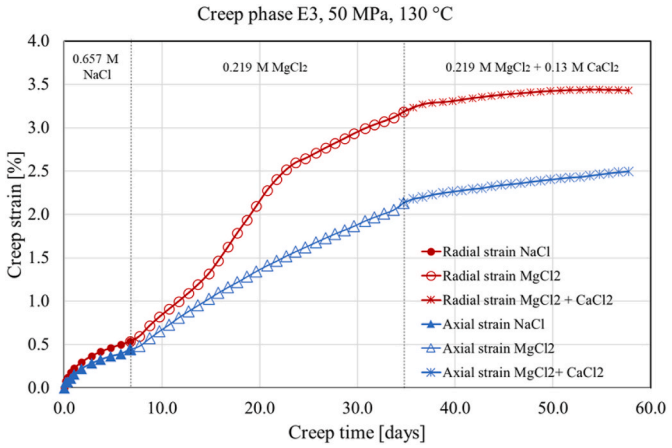

Fig. 5. Axial strain (blue lines) and radial strain (red lines) for core E3 during NaCl injection (filled markers), $MgCl_2$ (empty markers) and $MgCl_2$ spiked with $CaCl_2$ (cross markers) during creep at 50 MPa hydrostatic stress. (For interpretation of the references to colour in this figure legend, the reader is referred to the Web version of this article.)

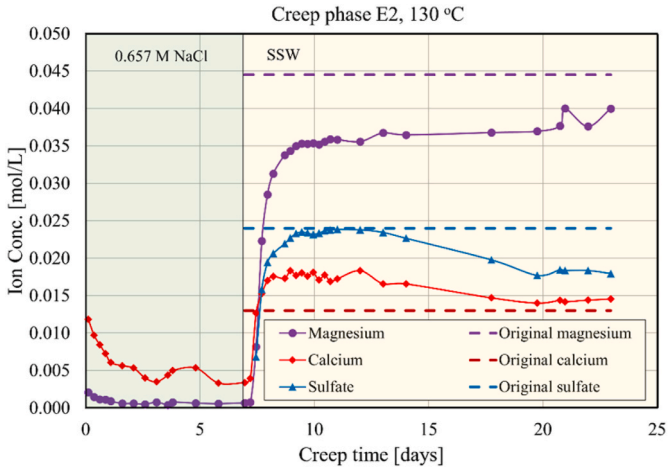

Fig. 6. Magnesium (purple line), calcium (red line) and sulfate (blue line) concentrations of effluents [mol/L] during creep time [days] and flooding of inert (green shade) and reactive (yellow shade) brines of core E2. Dashed lines indicate original ion concentrations. (For interpretation of the references to colour in this figure legend, the reader is referred to the Web version of this article.)

Magnesium loss was detected throughout Synthetic Seawater (SSW) flooding, in comparison to the original brine concentration; the magnesium concentration in the effluent increased to 0.035 mol/L in the first 6 PVs transitioning from NaCl injection. For the rest of the creep phase, the concentration increased slowly, up to 0.04 mol/L, but remained clearly below the injected concentration, by approximately 11%.

Excess calcium is produced during SSW injection, and the effluent calcium concentration showed an increasing trend up to 0.018 mol/L, from day 8 to day 10, exceeding the injected concentration of 0.013 mol/L, Thereafter, a decrease in the calcium concentration down to ~0.014 mol/L at day 20 was found, where it stabilized over the last three creep days, still 0.001 mol/L above the original concentration of 0.013 mol/L.

The sulfate concentration in the effluent (Fig. 6, blue lines) reached the original SWW concentration after two days of SSW injection. Later during creep (from day 13) the sulfate concentration started a decreasing trend for the next 7 days, finally stabilizing around 25% below the injected concentration.

For core E3, the effluent profiles were based on the concentrations of magnesium (Mg^{2+}) and calcium (Ca^{2+}). When flooding with NaCl, the effluent concentrations of Na^+ and Cl^- were practically the same as the injected, i.e. 0.657 mol/L. A small calcium peak of 0.01 mol/Lwas found initially (Fig. 7, red line), but it rapidly went down to negligible values.

When changing from NaCl to $MgCl_2$, a transient behavior in calcium production and magnesium retention can be observed in Fig. 6 (red line, respectively purple line). A calcium peak starts, when introducing $MgCl_2$, from a concentration of ~0.003 mol/L before the production of calcium increases to a maximum value of 0.033 and stabilizes at 0.026 mol/L around day 10 of creep. This corresponded with loss of magnesium, as the concentration in the sampled effluent increased from 0 and stabilizes at ~0.190 mol/L, clearly below the injected concentration of 0.219 mol/L.

When 0.130 M $CaCl_2$ was added to the flooding brine in the period between 34 and 59 days of creep, an immediate response in the calcium production and magnesium retention occurred. As seen in Fig. 6, the produced calcium concentration increased and slightly exceeded 0.130 mol/L (by ~0.01 mol/L), then it gradually decreased over the next 15 days and the difference between the effluent calcium concentration and that of the injected brine became negligible. Complementary to the calcium profile, a large peak in the magnesium effluent concentration with a maximum value of 0.252 mol/L can be observed. Thereafter, the magnesium concentration decreased quickly (~1–2 days), but only slightly below (~0.01 mol/L) the injected concentration, unlike during the previous brine injection. After ~15 d the effluent concentration was practically identical to that of the injected.

Generally, the evolution of magnesium and calcium concentrations are mirrored, retention of magnesium corresponding closely to excess production of calcium. This in agreement with previous experimental studies (Madland et al., 2011; Megawati et al. 2011, 2015; Andersen et al., 2012, 2018; Minde et al., 2018) which show that when injecting brines containing reactive Ca and Mg ions, the dissolution of calcite and precipitation of magnesite can occur in a substitution-like way, as the moles Ca production is the same as moles Mg retention, as described by the reaction:

$$CaCO_3(s) + Mg^{2+}(aq) \leftrightarrow MgCO_3(s) + Ca^{2+}(aq).$$

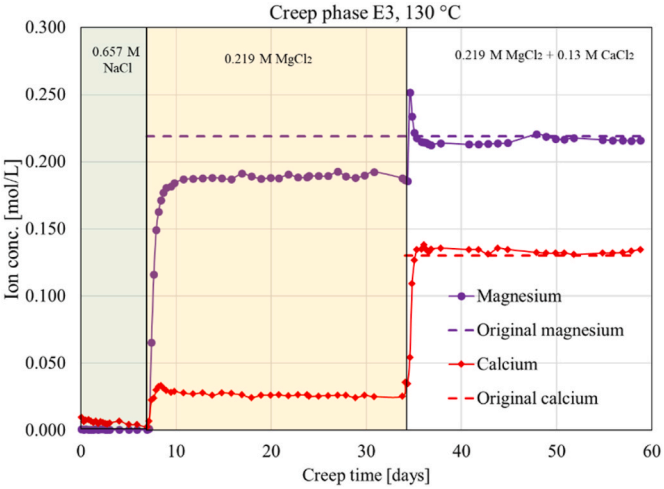

Fig. 7. Magnesium (purple line), calcium (red line) and sulfate (blue line) concentrations of effluents [mol/L] during creep time [days] and flooding with inert bine (green shade) magnesium chloride (yellow shade) and calcite-enhanced magnesium chloride (unshaded) of core E3. Dashed lines indicate original ion concentrations. (For interpretation of the references to colour in this figure legend, the reader is referred to the Web version of this article.)

3.3. Field emission Gun-Scanning Electron Microscopy (FEG-SEM) – core E3

Mineralogical and compositional analysis by Scanning Electron Microscopy (SEM) combined with Energy-dispersive X-ray spectroscopy (EDS) have been performed at the inlet of the Eldfisk core E3, which has been exposed to 81 PVs $MgCl_2$ and 75 PVs $MgCl_2$ + $CaCl_2$. FEG-SEM images from the flooded core are shown in Figs. 7 and 8. Chemical alteration is shown in Fig. 8 by the occurrence of newly formed minerals in open pore spaces, mostly inside foraminifer shells.

The crystals appear as trigonal aggregates and the EDS spectrum indicates a high magnesium content (Fig. 8, right). The sharp edges indicate in-situ, post-depositional precipitation. An unequivocal interpretation of the new mineral crystals is difficult because of their small sizes (~1 μm), although it is likely to assume they are magnesite, as precipitation of magnesite has been confirmed in several studies on outcrop chalk flooded with $MgCl_2$ brine (Zimmermann et al., 2015; Andersen et al., 2018; Wang et al., 2018; Minde et al., 2020).

In addition, the SEM image and the EDS analysis reveal the presence of flakey clay minerals containing both magnesium and silicon (Fig. 9, red circle). These Si–Mg-rich minerals are also interpreted to be newly grown clay minerals as a result of injection of Mg-rich brines, a process observed in outcrop chalk studies as well (Madland et al., 2011; Minde et al., 2018, 2020). The SEM micrograph in Fig. 9 also shows unbroken microfossils are still present, along with occurrence of clay minerals and quartz. A part of these clay minerals is believed to be kaolinite originally present in the core before flooding. This is indicated by the EDS analysis in Fig. 9 (right) which shows high aluminum and silicon weight percent around 23.4 and 24.3% respectively, in addition to minor occurrence of magnesium, ~0.3 wt %, that probably remained from flooding with $MgCl_2$.

4. Discussion

The results from geomechanical testing of Eldfisk reservoir chalk cores in controlled laboratory conditions give a unique insight into the compaction behavior of reservoir chalk exposed to thermo-chemical influence, under hydrostatic stress conditions. A direct comparison between this study and the outcrop chalk experiments is difficult, given that the test parameters are not identical (i.e., different stress values, test time). However, under hydrostatic stress conditions, at 130 °C and exposed to chemical perturbation, generally Eldfisk reservoir chalk showed similar behavior as outcrop chalk described in Madland et al. (2011); Megawati et al. (2011); Korsnes et al. (2013); Megawati et al. (2015); Zimmermann et al. (2015); Andersen et al. (2018); Minde et al. (2018); Nermoen et al. (2018); Wang et al. (2018); Sachdeva et al. (2019a) in terms of mechanical and chemical response. This not only validates such experiments on outcrop chalk as relevant for reservoir chalk, but it also confirms the observations made by Sachdeva et al. (2019b), that the initial wettability of the chalk cores was inconsequential regarding the effect of the imposed fluids on the mechanical behavior of chalk. The presence of hydrocarbons in the cores used in this study did not seem to hinder the water weakening effect, indicating that application of rock-fluid interactions observed in water-wet experiments can be valid also in a reservoir context.

4.1. Mechanical behavior in hydrostatic loading phase

Hydrostatic loading caused a linear stress-strain relationship in both tests, E2 and E3, and neither of the cores yielded, i.e., the deformation rate did not increase in respect to the hydrostatic loading rate. Madland et al. (2011) reported yield point at approximately 8 MPa for outcrop chalk from Liège under the same stress and thermochemical conditions (hydrostatic stress, NaCl at 130 °C). The difference in yielding behavior may be related to chalk porosity (41% in Madland et al., 2011 tests compared to 18–19% in this study) as chalk's mechanical strength increases with decreasing porosity (Risnes and Flaageng, 1999). Also, the nature of the saturation fluid can influence the core stiffness (Sachdeva et al., 2019b), so that the presence of residual oil in may have stiffened the reservoir cores.

However, a non-linear stress-strain behavior is observed in the beginning of the loading at approximately 15 MPa (Fig. 10) where the strain rate decreases and the stress-strain linearity slope increases by 23% for core E2 and 44% for core E3. This could be related to the condition of the cores, as commonly noticed in rocks under large stresses (Fjær et al., 2008), especially in rocks that contain fine/small-scale cracks. As the confining pressure increases, the fine cracks are compressed, resulting in a relatively higher initial strain. As the crack aperture closes, the compression of the core becomes more difficult, thus, the rate of deformation becomes lower promoting a new elastic phase of linear stress-strain from which the bulk modulus is estimated.

Although the test conditions were the same for both cores (same hydrostatic loading rate, NaCl injection at 130 °C) the bulk modulus (*K*-modulus) differs between the two cores (3.9 GPa for E2 and 2.8 GPa

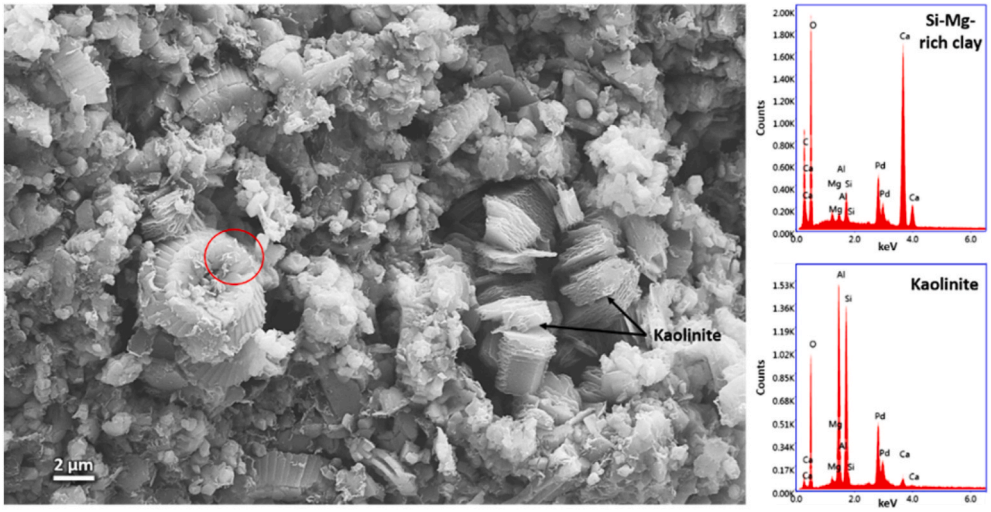

Fig. 8. SEM micrograph of flooded E3 containing fibrous Si–Mg-rich minerals precipitated on cocolith surfaces (red circle) and most likely kaolinite growth inside foraminifer cavity; Right: EDS analysis of these two mineral phases. (For interpretation of the references to colour in this figure legend, the reader is referred to the Web version of this article.)

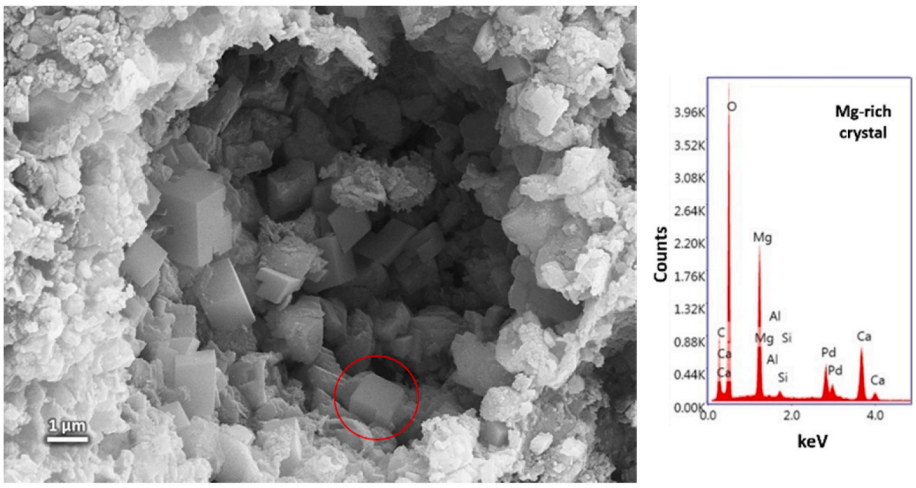

Fig. 9. Left: SEM micrograph of flooded chalk fragment from the inlet of core E3; red circle shows Mg-rich crystal. Right: EDS spectrum of the encircled crystal, possibly magnesite. (For interpretation of the references to colour in this figure legend, the reader is referred to the Web version of this article.)

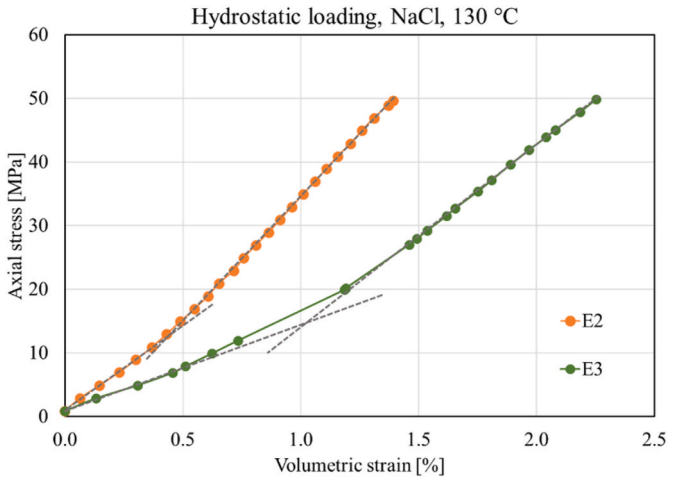

Fig. 10. Change in axial stress [MPa] - volumetric strain [%] relationship during hydrostatic loading.

for E3). The lower bulk modulus of E3 at the end of the loading phase also corresponds to a higher radial strain compared to E2, by a factor of 2.3, which contributed to a lower volumetric strain rate. This can be related to a brief, abrupt piston pressure cycle during test setup, when the piston pressure jumped from 0.55 MPa to 4.8 MPa, as the piston touched the core. This could have caused an expansion of the core diameter and axial compaction. The difference in radial strain between the two cores may also be related to the closure of fissures during hydrostatic loading; given that the two cores had almost the same initial effective porosity, this may be an indication that core E3 contained larger or more vertical fissures than core E2. The observation that the discrepancy in radial strain was evident only during loading phase, with increasing confining pressure, also supports this suggestion; during the first approximately 7 days of creep, when the stress was kept constant and before changing the injecting brine, the radial strain was comparable between the two cores. However, since both cores generally show the similar response to stress and brine chemistry, suggests that for this type of test, where the focus is primarily on the qualitative assessment of the results, the initial physical condition of the cores was not of essence.

Although the cores did not yield, despite the high confining pressure (50 MPa), their deformation was not elastic, as the accumulated strain during testing was irreversible. The estimated volumetric strain after unloading was approximately 5% for E2 and 8% for E3.

4.2. Effect of NaCl injection during creep

During flooding of E2 and E3 with NaCl, ion chromatograph analysis detected dissolution of calcite in the beginning of the creep phase (Figs. 11 and 12). Thereafter, the calcium concentration in the effluents decreased down to 0.003 mol/L in both tests before changing the injected brine, implying that NaCl is weakly reactive towards the chalk surface. However, the interaction between chalk and NaCl is negligible and comparable to observations from Nermoen et al. (2016) and Andersen et al. (2018) where the concentration of produced calcium when flooding NaCl through outcrop chalk cores at 130 °C stabilized between 0.002 and 0.004 mol/L.

The deformation during the first approximately 7 days of hydrostatic creep follows a typical curve for porous rocks (Figs. 11 and 12, black dotted line). The transient (primary) creep, recognized by a diminishing deformation rate, is followed by steady state deformation (secondary creep), where the strain rate is constant. An acceleration of strain rate may occur over time, (tertiary creep), usually associated with high effective stresses, which leads rapidly to core failure (Hudson, 1993; Fjær et al., 2008). However, this is not the case here. The cores did not

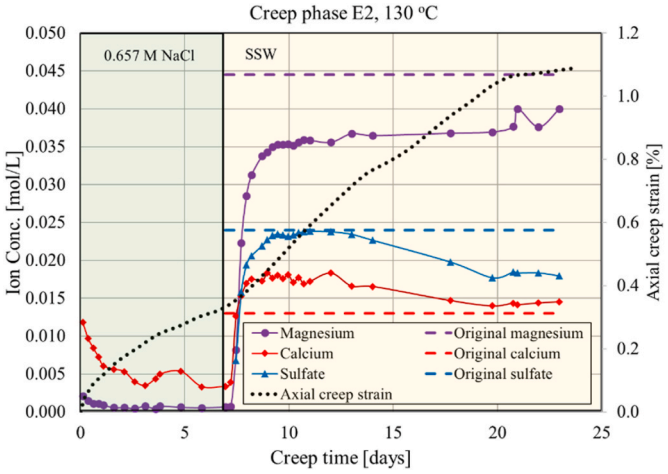

Fig. 11. Axial deformation (dotted black line) and magnesium (purple line), calcium (red line) and sulfate (blue line) concentrations of effluents [mol/L] during creep time [days] and flooding inert (green shade) and reactive (yellow shade) brine of core E2. Dashed lines indicate original ion concentrations. (For interpretation of the references to colour in this figure legend, the reader is referred to the Web version of this article.)

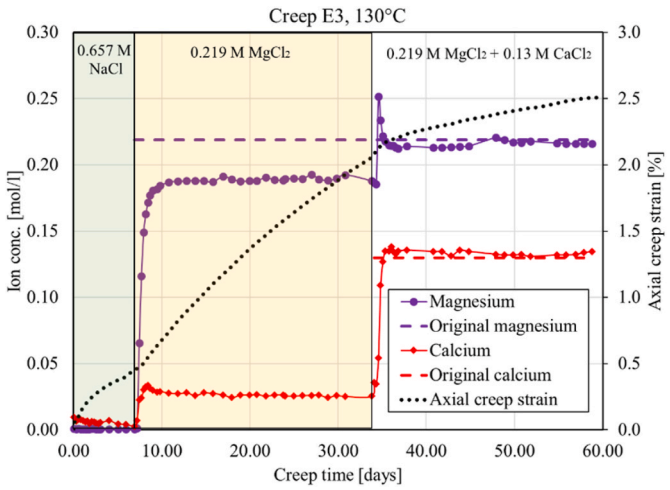

Fig. 12. Axial deformation (dotted black line) and magnesium (purple line) and calcium (red line) concentrations of effluents [mol/L] during creep time [days] and flooding inert brine (green shade) magnesium chloride (yellow shade) and calcite-enhanced magnesium chloride (unshaded) of core E3. Dashed lines indicate original ion concentrations. (For interpretation of the references to colour in this figure legend, the reader is referred to the Web version of this article.)

fail, indicating that the increasing deformation rate observed in both tests after changing injecting brines is not related to chalk poroelastic behavior. Since the test setup provides that other test parameters that could influence strain rate, such as stress, temperature, or brine injection rate (Nermoen et al., 2016; Sachdeva et al., 2019 b) remain the same throughout the creep phase, the change in strain rate can only be the result of the change of injecting brine composition.

4.3. Effect of SSW injection during creep

The effect of the major divalent ions i.e. magnesium, calcium and sulfate, on the mechanical response of the Eldfisk core E2, have been emphasized during the continuous flow of seawater throughout the creep phase. In Fig. 11, both the axial creep strain (dotted black line) and the concentrations of the surface active ions in seawater (Mg^{2+}, Ca^{2+}, and SO_4^{2-}) present in the effluents are plotted versus creep time for core E2.

The core's axial creep rate increases compared to when injected with NaCl, while at the same time magnesium ions are retained in the core and calcium ions are produced. The excess calcium and the loss of magnesium can be explained by dissolution of calcite and precipitation of magnesium-bearing minerals, seemingly the ongoing processes during seawater injection.

Additionally, the decrease in concentration of sulfate ions when flooding the core with seawater at 130 °C, together with clogging in the outlet steel tubing after ~20 days of SSW injection, point toward the precipitation of new minerals such as anhydrite, $CaSO_4$ (Heggheim et al., 2005; Hiorth et al., 2008; Madland et al., 2008). Also, the sum of measured magnesium concentration and the additional amount of calcium ions in the effluent are lower than the magnesium concentration of the injected brine, i.e. 0.0445 mol/L, which can confirm the occurrence of anhydrite precipitation (Madland et al., 2011). Due to anhydrite formation, the fluid in the pores would be undersaturated with respect to calcium, which promotes calcite dissolution.

4.4. Effect of $MgCl_2$ injection during creep

$MgCl_2$ represents a simplified aqueous chemistry of seawater, and it is injected specially to investigate the effect of magnesium ions on the mechanical strength of chalk. When core E3 is injected with $MgCl_2$, after switching from NaCl, a clear physical response is observed. The chemically induced creep deformation is reflected in the plot of axial strain along (dotted black line) with the effluent concentration profiles as a function of creep time in Fig. 12.

A steady considerable amount of excess calcium (red line) was produced, approximately 0.026 mol/L, while a substantial amount of magnesium (purple line) was retained in the core (approximately 0.03 mol/L) as the $MgCl_2$ flooding commenced. This calcium production, indicative of calcite dissolution is significantly higher than that observed during NaCl injection and it is in the same range as the calcium production described in Andersen et al. (2018) from experiments on outcrop chalk from Liège, Mons (Belgium) and Stevns Klint (Denmark).

At the same time, the axial strain rate increased (Fig. 12, dotted line) as a response to the non-equilibrium nature of the rock-fluid interface. Chemically induced deformation has been observed in multiple earlier studies on outcrop chalk (Madland et al., 2008, 2011; Megawati et al., 2015; Andersen et al., 2018; Minde et al., 2018; Wang et al., 2018) which explain it as a result of calcite dissolution enhanced by precipitation of magnesium-bearing minerals.

This is seen here as well, newly precipitated magnesium-bearing minerals also having been detected in the inlet of E3 by SEM-EDS analysis (Fig. 8). Although not clearly identified, due to their minute size, these newly precipitated crystals are most likely magnesite, agreeing to previous studies on outcrop chalk at similar conditions (Korsnes et al., 2013; Zimmermann et al., 2015; Minde et al., 2018). Magnesium-rich minerals have higher densities than calcite, thereby, less volume is occupied in the core as magnesite and other magnesium-bearing minerals precipitate at the expense of calcite. This is likely to contribute to the enhancement of creep strain. However, future studies comparing the mineral and geochemical composition of the cores before and after testing will allow a more comprehensive evaluation of the physical and compositional changes induced by the rock-fluid interactions.

4.5. Effect of adding $CaCl_2$ to $MgCl_2$

Adding $CaCl_2$ to $MgCl_2$ produced a similar effect as described in Megawati et al. (2011). Fig. 12 shows that as soon as $CaCl_2$ is added to the $MgCl_2$ brine, the magnesium (purple line) and calcium concentrations (red line) lay steady around the original ion concentrations of the injected brine, together with a clear reduction in creep compaction rate (dotted black line). Andersen and Berawala (2019) explained this phenomenon by mathematical modeling where the creep compaction was driven both by a stress component and a dissolution rate component. Reducing or eliminating the dissolution rate would result in strongly reduced compaction rate, but not a full stop. Accordingly, the compaction reduction here was clear, but not as severe as seen in the study by Megawati et al. (2011) on outcrop chalk (Liège, Gulpen Fm) where the deformation nearly ceased. This may be due to textural differences between the two chalk cores or the different test parameters (creep stress at 11.6 MPa in Megawati et al., 2011 compared to 50 MPa in this study, and over different periods of time).

5. Conclusions

Hydrostatic loading and creep compaction with continuous brine injection was performed on two Eldfisk reservoir chalk cores. The ion concentrations of the effluent water samples have been analyzed chemically, and a sample from the inlet of the core flooded with magnesium chloride brines has been analyzed by SEM-EDS. Thereafter, the geomechanical behavior of Eldfisk cores have been compared with previous results obtained from onshore outcrop chalks. The main conclusions can be summarized as follows:

- Production of excess calcium and retention of magnesium while flooding seawater-like brines are explained by of dissolution of

primary calcite and precipitation of secondary Mg-bearing minerals. It is probable that the retention of sulfate ions in SSW enables anhydrite precipitation.

- Dissolution and precipitation processes seem to be key driving mechanisms for chemical creep compaction in the flooding experiments of reservoir core chalk.
- The creep deformation rate depended on the flooding brine: SSW and $MgCl_2$ injection caused excess production of calcium (calcite dissolution) which correlated with enhanced water weakening of Eldfisk cores compared to when flooding NaCl brine. Adding calcium to $MgCl_2$ stopped calcium production, which resulted in clear attenuation of the creep strain.
- The Eldfisk reservoir chalk cores behaved in a comparable manner to outcrop cores under similar test conditions (stress and thermochemical exposure) in terms of rock-fluid interactions (such as dissolution and precipitation processes as mentioned above) and geo-mechanical behavior (i.e., water weakening), despite the natural differences between the chalk types (depositional environments, stress history, diagenetic grade, mineralogy) and the wettability phase. This indicates that observations of the effect of water-weakening mechanisms on outcrop chalk can also be valid for reservoir chalk.

Author credit statement

Emanuela Kallesten: Conceptualization, Investigation, interpretation, data visualization, writing. Yosra Cherif: Conceptualization, Investigation, interpretation, analyses, review. Merete V. Madland: Supervision, sample provision, Conceptualization, Validation, review and editing. Reidar I. Korsnes: Conceptualization, Supervision, interpretation, review and editing. Edvard Omdal: Supervision, resources provision, Conceptualization, review and editing. Pål. Ø. Andersen: Supervision, critical review, revision commentaries, Visualization. Udo Zimmermann: Supervision, Conceptualization, review and editing.

Declaration of competing interest

The authors declare that they have no known competing financial interests or personal relationships that could have appeared to influence the work reported in this paper.

Acknowledgement

The authors acknowledge the Research Council of Norway and the industry partners, ConocoPhillips Skandinavia AS, Aker BP ASA, Vår Energi AS, Equinor ASA, Neptune Energy Norge AS, Lundin Norway AS, Halliburton AS, Schlumberger Norge AS, and Wintershall DEA, of The National IOR Centre of Norway for support.

Appendix A. Supplementary data

Supplementary data to this article can be found online at https://doi.org/10.1016/j.petrol.2020.108164.

References

Ahsan, R., Fabricius, I.L., 2010, June. Sorption of magnesium and sulfate ions on calcite. In: 72nd EAGE Conference and Exhibition-Workshops and Fieldtrips. European Association of Geoscientists & Engineers cp-161.

Andersen, P Ø, Evje, S, Madland, M V, Hiorth, A, et al., 2012. A geochemical model for interpretation of chalk core flooding experiment. Chem. Eng. Sci. 84, 218–241.

Andersen, P.Ø., Wang, W., Madland, M.V., Zimmermann, U., Korsnes, R.I., Bertolino, S. R.A., et al., 2018. Comparative study of five outcrop chalks flooded at reservoir conditions: chemo-mechanical behaviour and profiles of compositional alteration. Transport Porous Media 121 (1), 135–181.

Andersen, P.Ø., Berawala, D.S., 2019. Modeling of creep-compacting outcrop chalks injected with Ca-Mg-Na-Cl brines at reservoir conditions. SPE J.

Brasher, J.E., Vagle, K.R., 1996. Influence of lithofacies and diagenesis on Norwegian North Sea chalk reservoirs. AAPG Bull. 80 (5), 746–768.

Collin, F., Cui, Y.J., Schroeder, C., Charlier, R., 2002. Mechanical behaviour of Lixhe chalk partly saturated by oil and water: experiment and modelling. Int. J. Numer. Anal. Methods GeoMech. 26 (9), 897–924.

Cook, C.C., Brekke, K., 2004. Productivity preservation through hydraulic propped fractures in the Eldfisk North Sea chalk field. SPE Reservoir Eval. Eng. 7, 105–114, 02.

Fabricius, I.L., Borre, M.K., 2007. Stylolites, porosity, depositional texture, and silicates in chalk facies sediments. Ontong Java Plateau–Gorm and Tyra fields, North Sea. Sedimentology 54 (1), 183–205.

Fjær, E., Holt, R.M., Horsrud, P., Raaen, A.M., Risnes, R., 2008. In: Petroleum Related Rock Mechanics, second ed., vol. 53 50;257.

Gautier, J.M., Oelkers, E.H., Schott, J., 2001. Are quartz dissolution rates proportional to BET surface areas? Geochem. Cosmochim. Acta 65 (7), 1059–1070.

Heggheim, T., Madland, M.V., Risnes, R., Austad, T., 2005. A chemical induced enhanced weakening of chalk by seawater. J. Petrol. Sci. Eng. 46 (3), 171–184.

Hermansen, H., Thomas, L.K., Sylte, J.E., Aasboe, B.T., 1997, January. Twenty five years of Ekofisk reservoir management. In: SPE Annual Technical Conference and Exhibition. Society of Petroleum Engineers.

Hermansen, H., Landa, G.H., Sylte, J.E., Thomas, L.K., 2000. Experiences after 10 years of waterflooding the Ekofisk field, Norway. J. Petrol. Sci. Eng. 26 (1–4), 11–18.

Hiorth, A., Cathles, L.M., Kolnes, J., Vikane, O., Lohne, A., Madland, M.V., 2008, October. Chemical modelling of wettability change in carbonate rocks. In: 10th Wettability Conference, pp. 1–9. Abu Dhabi, UAE.

Hiorth, A., Cathles, L.M., Madland, M.V., 2010. The impact of pore water chemistry on carbonate surface charge and oil wettability. Transport Porous Media 85 (1), 1–21.

Hjuler, M.L., Fabricius, I.L., 2007. Diagenetic Variations between Upper Cretaceous Outcrop and Deeply Buried Reservoir Chalks of the North Sea Area. AAPG 2007 Annu. Conv. Exhib.

Hjuler, M.L., Fabricius, I.L., 2009. Engineering properties of chalk related to diagenetic variations of Upper Cretaceous onshore and offshore chalk in the North Sea area. J. Petrol. Sci. Eng. 68 (3–4), 151–170.

Hudson, J.N., 1993. In: Comprehensive Rock Engineering, Principals, Practice and Projects, Volume 3, Rock Testing and Site Characterization. Pergamon Press, Oxford, pp. 119–121.

Japsen, P., 1998. Regional velocity-depth anomalies, North Sea Chalk: a record of overpressure and Neogene uplift and erosion. AAPG Bull. 82 (11), 2031–2074 japsen.

Japsen, P., Bidstrup, T., 1999. Quantification of late Cenozoic erosion in Denmark based on sonic data and basin modelling. Bull. Geol. Soc. Den. 46, 79–99.

Japsen, P., 2000. Fra Kridthav til Vesterhav. Nordsøbassinets udvikling vurderet ud fra seismiske hastigheder. Change 24, 165–173.

Jarvis, I., 2006. The Santonian-Campanian phosphatic chalks of England and France. Proc. Geologists' Assoc. 117 (2), 219–237.

Kallesten, E.I., Andersen, P.Ø., Madland, M.V., Korsnes, R.I., Omdal, E., Zimmermann, U., 2020a. Permeability evolution of shear failing chalk cores under thermochemical influence. ACS Omega 5 (16), 9185–9195.

Kallesten, E., Andersen, P.Ø., Berawala, D.S., Korsnes, R.I., Madland, M.V., Omdal, E., Zimmermann, U., 2020b. Modeling of permeability and strain evolution in chemical creep compaction experiments with fractured and unfractured chalk cores conducted at reservoir conditions. Soc. Petrol. Eng. SPE Journal. SPE-197371-PA.

Korsnes, R.I., Madland, M.V., Austad, T., 2006, April. Impact of brine composition on the mechanical strength of chalk at high temperature. In: Eurock, pp. 133–140.

Korsnes, R.I., Zimmermann, U., Madland, M.V., Bertolino, S.A.R., Hildebrand-Habel, T., Hiorth, A., 2013, November. Tracing fluid flow in flooded chalk under long term test conditions. In: First EAGE West Africa Workshop 2013-Subsurface Challenges in West Africa. European Association of Geoscientists & Engineers cp-348.

Madland, M.V., Midtgarden, K., Manafov, R., Korsnes, R.I., Kristiansen, T., Hiorth, A., 2008, October. The effect of temperature and brine composition on the mechanical strength of Kansas chalk. In: International Symposium SCA.

Madland, M.V., Hiorth, A., Omdal, E., Megawati, M., Hildebrand-Habel, T., Korsnes, R.I., et al., 2011. Chemical alterations induced by rock–fluid interactions when injecting brines in high porosity chalks. Transport Porous Media 87 (3), 679–702.

Madsen, H.B., 2010. Silica diagenesis and its effect on porosity of upper Maastrichtian chalk–an example from the Eldfisk Field, the North Sea. Bull. Geol. Soc. Den. 20, 47–50.

Megawati, M., Andersen, P.Ø., Korsnes, R.I., Evje, S., Hiorth, A., Madland, M.V., 2011. The effect of aqueous chemistry ph on the time-dependent deformation behaviour of chalk experimental and modelling study. Pore2Fluid IFP Energies Nouvel. Paris 16–18. Nov.

Megawati, M., Hiorth, A., Madland, M.V., 2013. The impact of surface charge on the mechanical behavior of high-porosity chalk. Rock Mech. Rock Eng. 46 (5), 1073–1090.

Megawati, M., Madland, M.V., Hiorth, A., 2015. Mechanical and physical behavior of high-porosity chalks exposed to chemical perturbation. J. Petrol. Sci. Eng. 133, 313–327.

Minde, M.W., Zimmermann, U., Madland, M.V., Korsnes, R.I., Schulz, B., Audinot, J.N., 2016, August. Fluid–flow during EOR experiments in chalk: insights using SEM–MLA, EMPA and Nanosims Applications. In: International Symposium of the Society of Core Analysts, pp. 21–26. Colorado, USA.

Minde, M.W., Wang, W., Madland, M.V., Zimmermann, U., Korsnes, R.I., Bertolino, S.R., Andersen, P.Ø., 2018. Temperature effects on rock engineering properties and rock-fluid chemistry in opal-CT-bearing chalk. J. Petrol. Sci. Eng. 169, 454–470.

Minde, M.W., Zimmermann, U., Madland, M.V., Korsnes, R.I., Schulz, B., Gilbricht, S., 2020. Mineral replacement in long-term flooded porous carbonate rocks. Geochem. Cosmochim. Acta 268, 485–508.

Nermoen, A., Korsnes, R.I., Hiorth, A., Madland, M.V., 2015. Porosity and permeability development in compacting chalks during flooding of nonequilibrium brines: insights from long-term experiment. J. Geophys. Res.: Solid Earth 120 (5), 2935–2960.

Nermoen, A., Korsnes, R.I., Aursjø, O., Madland, M.V., Kjørslevik, T.A., Østensen, G., 2016. How stress and temperature conditions affect rock-fluid chemistry and mechanical deformation. Front. Phys. 4, 2.

Nermoen, A., Korsnes, R.I., Storm, E.V., Stødle, T., Madland, M.V., Fabricius, I.L., 2018. Incorporating electrostatic effects into the effective stress relation—insights from chalk experiments. Geophysics 83 (3), MR123–MR135.

Puntervold, T., Austad, T., 2008. Injection of seawater and mixtures with produced water into North Sea chalk formation: impact of fluid–rock interactions on wettability and scale formation. J. Petrol. Sci. Eng. 63 (1–4), 23–33.

Risnes, R., Flaageng, O., 1999. Mechanical properties of chalk with emphasis on chalk-fluid interactions and micromechanical aspects. Oil Gas Sci. Technol. 54 (6), 751–758.

Sachdeva, J.S., Muriel, H., Nermoen, A., Korsnes, R.I., Madland, M.V., 2019 a. Chalk surface area evolution during flow of reactive brines: does oil play a role? Energy Fuel. 33 (6), 4890–4908.

Sachdeva, J.S., Nermoen, A., Korsnes, R.I., Madland, M.V., 2019 b. Impact of initial wettability and injection brine chemistry on mechanical behaviour of Kansas chalk. Transport Porous Media 128 (2), 755–795.

Scholle, P.A., 1977. Chalk diagenesis and its relation to petroleum exploration: oil from chalks, a modern miracle? AAPG (Am. Assoc. Pet. Geol.) Bull. 61 (7), 982–1009.

Schroeder, C., Bois, A.P., Maury, V., Halle, G., 1998, January. Water/chalk (or collapsible soil) interaction: Part II. Results of tests performed in laboratory on Lixhe chalk to calibrate water/chalk models. In: SPE/ISRM Rock Mechanics in Petroleum Engineering. Society of Petroleum Engineers.

Strand, S., Hjuler, M.L., Torsvik, R., Pedersen, J.I., Madland, M.V., Austad, T., 2007. Wettability of chalk: impact of silica, clay content and mechanical properties. Petrol. Geosci. 13 (1), 69–80.

Sulak, A.M., Danielsen, J., 1988, January. Reservoir aspects of Ekofisk subsidence. In: *Offshore Technology Conference*. Offshore Technology Conference.

Teufel, L.W., Rhett, D.W., Farrell, H.E., 1991. Effect of reservoir depletion and pore pressure drawdown on in situ stress and deformation in the Ekofisk field, North Sea. In: The 32nd US Symposium on Rock Mechanics (USRMS). American Rock Mechanics Association. January.

Wang, W., Madland, M.V., Zimmermann, U., Nermoen, A., Korsnes, R.I., Bertolino, S.R., Hildebrand-Habel, T., 2018. Evaluation of porosity change during chemo-mechanical compaction in flooding experiments on Liege outcrop chalk. Geol. Soc. Londn. Special Publ. 435 (1), 217–234.

Zimmermann, U., Madland, M.V., Nermoen, A., Hildebrand-Habel, T., Bertolino, S.A., Hiorth, A., et al., 2015. Evaluation of the compositional changes during flooding of reactive fluids using scanning electron microscopy, nano-secondary ion mass spectrometry, x-ray diffraction, and whole-rock geochemistry Compositional Changes during Flooding. AAPG (Am. Assoc. Pet. Geol.) Bull. 99 (5), 791–805.